Unraveling the auxin mechanism in 2,4-D induced somatic embryogenesis in Arabidopsis thaliana

Philipsen, C.

Chapter 3

Auxin dynamics during SE initiation is established by the tryptophan-dependent indole-3-pyruvic acid pathway in *Arabidopsis*.

Cheryl Philipsen[1],
Kadir Akdeniz[1,3],
Paulina Zwijnenburg[1],
Remko Offringa[1]

[1] *Molecular and Developmental Genetics, Institute of Biology Leiden, Leiden University, Sylviusweg 72, 2333BE, Leiden, the Netherlands*
[2] *Current affiliation: Dümmen Orange, P.O. Box 26, 2678ZG, de Lier, the Netherlands*
[3] *Current affiliation: Erasmus MC, 's-Gravendijkwal 230, 3015 CE Rotterdam*

Abstract

Somatic embryogenesis (SE) in *Arabidopsis* can be efficiently induced by treatment of immature zygotic embryos (IZEs) with the synthetic auxin analog 2,4-dichlorophenoxyacetic acid (2,4-D). The exact involvement of the natural auxin, indole acetic acid (IAA), and its biosynthesis in 2,4-D-induced SE initiation is yet to be solved. IAA is mostly produced in the root and shoot apical meristem via L-tryptophan (Trp)-dependent or -independent pathways. The best-characterized Trp-dependent pathway is the indole-3-pyruvic acid (IPyA) pathway, which includes two enzymatic steps that successively convert Trp into IPyA and IPyA to IAA. The first step comprises the TRYPTOPHAN AMINOTRANSFERASE OF ARABIDOPSIS1 / TRYPTOPHAN AMINOTRANSERASE RELATED1-4 (TAA1/TAR1-4) family of enzymes. The second step includes the YUCCA1-11 (YUC1-11) family enzymes. We used combinations of chemical biology, genetics and reporter studies to unravel the Trp-dependent pathway during 2,4-D induced SE initiation. Our results suggest that YUC activity is rather required for development of the embryo and that TAA1/TARs are required to establish a dynamic auxin response to initiate SE.

Introduction

The plant hormone auxin, or indole-3-acetic acid (IAA), controls many aspects of plant development, from early zygotic embryogenesis to later patterning events such as leaf venation and phyllotaxis (Sawchuk and Scarpella, 2015; Reinhardt et al., 2003). The discovery of auxin, its activity and auxin-like compounds have led to the application and many uses of auxins in research and tissue culture (De Rybel et al., 2009; Song, 2014). The natural auxins IAA and indole-butyric-acid (IBA) and synthetic auxin analogs 1-naphthaleneacetic acid (1-NAA) and 2,4-dichlorophenoxyacetic acid (2,4-D) are abundantly used in tissue culture to induce rooting on plant cuttings, or to obtain plant regeneration by induction of callus, shoots or even embryos on vegetative plant tissues (Gaj, 2001; Su and Zhang, 2014). The latter process, referred to as somatic embryogenesis, in most cases requires long-term incubation of competent plant tissues on 2,4-D (Su and Zhang, 2014). In *Arabidopsis*, somatic embryos can be efficiently induced by incubating immature zygotic embryos on 2,4-D-containing SE induction medium (SEIM). Although this protocol was established some time ago (Gaj, 2001; Nowak et al., 2012), the mechanism by which 2,4-D induces SE initiation and acts on endogenous IAA biosynthesis in this process, has not been elucidated yet. Studies on the effect of 2,4-D on plant cells and tissues show that the auxin response is elevated (Pasternak, 2002; Michalczuk et al., 1992; Simon et al., 2013; Song, 2014) and in Chapter 2 we have shown that prior to SE initiation the auxin response is elevated followed by a local minimum in foci of embryogenic cells. This chapter focuses on the role of auxin biosynthesis in causing the subsequent 2,4-D-induced auxin response maxima and minima that lead to SE.

Auxin responses are tightly controlled by its biosynthesis and metabolism, transport and signaling. Auxin is produced mainly in developing tissues in the shoot and root and through polar auxin transport IAA is redistributed from the source to locations where IAA is required to steer plant development (Robert et al., 2015). Research in *Arabidopsis* and *Zea mays* (maize) has uncovered several IAA biosynthesis routes, which fall into two categories: the tryptophan (Trp)-dependent and the Trp-independent routes. Four Trp-dependent pathways have been uncovered and named after the intermediate compound produced using L-tryptophan (Trp) as a substrate: i) the indole-3-acetaldoxime (IAOx) pathway, ii) the indoleacetamide (IAM) pathway, iii) the tryptamine pathway (TAM) and iv) the indole-3-pyruvic acid (IPyA) pathway (Woodward and Bartel, 2005; Korasick et al., 2013; Ljung, 2013). Genetic and biochemical evidence indicates that the IPyA pathway, which includes a two-step enzymatic conversion of Trp to IAA, is the major auxin biosynthesis route in plants (Zhao et al., 2012). The first step

involves the TRYPTOPHAN AMINOTRANSFERASE OF ARABIDOPSIS1 / TRYPTOPHAN AMINOTRANSERASE RELATED 1-4 (TAA1/TAR1-4) family of enzymes that convert Trp to IPyA (Stepanova et al., 2011; Won et al., 2011; Tao et al., 2008). In the second step the YUCCA (YUC) family of proteins convert IPyA to IAA (Zhao et al., 2001; Cheng, 2006; Cheng et al., 2007).

Mutations in the *TAA1* gene and its closest homologs *TAR1* and *TAR2* result in altered meristem functioning, defects in flowering and embryo development (Stepanova et al., 2008). The *wei8 tar1 tar2* triple mutants display *monopteros* (*mp*)-like phenotypes: they fail to establish the basal part of the embryo and often develop a single cotyledon (Stepanova et al., 2008). The quadruple mutant *yuc1 yuc4 yuc10 yuc11* displays similar phenotypes as the triple *wei8 tar1 tar2* mutant (Cheng, 2006; Cheng et al., 2007). More embryonic defects were discovered in knock out combinations of *yuc3*, *yuc4*, and *yuc9*. Local auxin production was proposed to act in conjunction with PIN-FORMED1 (PIN1) driven polar auxin transport to establish auxin gradients that steer pattern development in the *Arabidopsis* embryo (Robert et al., 2013).

Despite sufficient genetic evidence that the IPyA auxin biosynthesis route is important for zygotic embryogenesis in *Arabidopsis*, its role in 2,4-D-induced SE has only superficially been touched. In an *Arabidopsis* 2,4-D-induced secondary SE culture system (Bai et al., 2013) expression of *YUC1*, *YUC2*, *YUC4*, *YUC6* was shown to be enhanced following SE initiation by transfer of embryonic calli to 2,4-D free medium. In this system, single and higher order mutants of *yuc1, yuc2, yuc4,* and *yuc6* were not affected in their SE capacity. In contrast, *yuc1 yuc4 yuc10 yuc11* quadruple mutant embryonic calli showed a significant reduction in the SE capacity (Bai et al., 2013). A major disadvantage of the secondary SE culture system is that somatic embryos are derived from pre-existing embryonic calli in the absence of 2,4-D (Nowak et al., 2012), and therefore the early events that lead to the induction of embryo identity by 2,4-D cannot be studied.

Here, we studied the role of auxin biosynthesis in our primary 2,4-D induced SE on *Arabidopsis* IZEs, first by using two chemical inhibitors, L-kynurenine (kyn) (He et al., 2011) and yucasin (yuc) (Nishimura et al., 2014) that respectively block the Trp → IPyA and IPyA → IAA conversions, and secondly by studying the effect of loss-of-function mutations and the expression of *TAA/TAR* and *YUC* genes during 2,4-D induced SE. Surprisingly, our data shows that the YUCCA-mediated IPyA → IAA conversion is not required for SE initiation, but only for later development of the somatic embryos, whereas the Trp → IPyA conversion step, as regulated by TAA1/TARs enzymes, is crucial for this process.

Results

YUCCAs are not essential for SE initiation, but are required for somatic embryo development

Based on the results of Bai and coworkers (2013) suggesting the important role of the *YUC* genes in 2,4-D-induced SE initiation, we tested the inhibitor yucasin, which specifically blocks the IPyA → IAA conversion by the YUCCA monooxygenases, in our primary *Arabidopsis* SE system. Earlier experiments showed that the first *pWOX2::YFP*-marked embryonic cells could be observed after 5 days, but not yet after 3 days of incubation on SEIM (Chapter 2). We have demonstrated in Chapter 2 that it was possible to identify at which stage an auxin related pathway has a role by applying chemical inhibitors prior (day 0), during (day 3) or after (day 5) the establishment of these first embryogenic cells. In previous control experiments (Chapter 2) we observed that the transfer to fresh SEIM medium does not affect SE. By applying 100µM yucasin we anticipated to be able to determine at which stage YUC activity would be important. Early yucasin application (day 0) reduced both SE efficiency (the frequency of IZEs producing somatic embryos) and -productivity (average number of somatic embryos produced per IZE) to 0 (Figure 1a), as all IZEs died within the first five days of culture (Figure 1b). Application of yucasin from day 3 onwards resulted in a mild but significant reduction of the SE efficiency (67% compared to 84% in the control), but the productivity was not affected (Figure 1a,b). Yucasin application on day 5 did not significantly affect the SE efficiency, but the SE productivity decreased from 1.4 to 0.5 SEs/IZE. Thus, the IPyA → IAA conversion step controlled by YUCCAs is important for the survival of the IZE in tissue culture, and plays a role during SE, however it is not crucial for SE initiation. The reduction in SE productivity following yucasin application at day 5 was the result of the appearance of more fused embryos (embryonic clusters) and shoot-like structures as opposed to individual somatic embryos in the yucasin treated IZEs as compared to control IZEs. As we are unaware of the stability of yucasin, we presume that it causes a stronger effect when freshly applied on day 5 during the embryo development phase. In conclusion, YUC activity is required for survival of IZEs and for proper development of induced embryonic cells into individual somatic embryos, but not for SE initiation.

To further study the effect of yucasin on 2,4-D treated IZEs, we used the *DR5::GUS* auxin response reporter (Ulmasov et al., 1997; Friml et al., 2003). IZEs of an *Arabidopsis DR5::GUS* line were incubated on SEIM for 4hr with or without 100µM yucasin, or on SEIM without 2,4-D and subsequently stained for GUS activity. As a control, IZEs were included that were freshly isolated from the ovule and

were directly stained for GUS activity. In the control IZEs, *DR5::GUS* was clearly expressed in the root and cotyledons tips and in provascular tissues in cotyledons and the hypocotyl, as described before (Friml et al., 2003).This expression pattern was more pronounced in the SEIM incubated IZEs (Figure 1c,d), and slightly weaker in the absence of 2,4-D, but significantly reduced when IZEs were incubated on SEIM with yucasin (Figure 1c,d). The most striking difference was that all SEIM incubated IZEs showed a strong *DR5::GUS* expression in the hypocotyl, whereas this was only observed in a few yucasin (11%), or hormone free SEIM (8%) treated IZEs (Figure 1d). The results confirm that short-term 2,4-D treatment enhances the auxin response, and that this enhancement is dependent on YUCCA-mediated auxin biosynthesis that is essential for IZE survival during the first few days on SEIM.

YUCCAs are involved in somatic embryo development

To confirm the role of *YUCCA* genes in IZE survival and somatic embryo development, we analyzed promoter reporter lines for several *YUCCAs* in IZEs that were incubated for 0, 3, 5 and 7 days on SEIM medium. Representative microscopy images and frequency of observations are shown in Figure S1 and Table S1 and a schematic representation of the expression observed in more than 20% of the IZEs tested is shown in Figure 2a. Since somatic embryos are mostly developing from the SAM or the proximal adaxial side of cotyledons of an IZE, we expected *YUCCA* genes directly involved in SE to be specifically induced in these tissues of the IZE on days 5 and 7. *YUC2* and *YUC10* were not or barely expressed in IZEs at any time point, in any tissue (Figure S1, Table S1). However, for *YUC4*, *YUC6*, *YUC8* and *YUC9* an interesting dynamic expression pattern was observed, suggesting their involvement in somatic embryo development. *YUC4* was weakly expressed in the epidermis throughout the IZE and more strongly in the SAM on day 0 and day 3 (Figure S1, Figure 2a). On day 5, expression was not observed in SE regions but was enhanced in the SAM and the cotyledon- and root tips, followed by its confinement to the SAM and the proximal region of the cotyledons on day 7. *YUC6* expression was confined to the provascular tissue of the IZE, starting at day 0, disappearing on day 3, and returning on day 5 with particularly strong expression below the areas of SE initiation on day 7. Since somatic embryos do not develop from the provascular tissue but from the epidermal layer (Raghavan, 2004; Kurczyńska et al., 2007) it is unlikely that *YUC6* is directly involved in SE. However, based on its temporal expression, it is likely to be important for IZE survival and somatic embryo development. *YUC8* and *YUC9* have a similar expression pattern in which expression on day 0, 3 and 5 is confined to the cotyledons tips. On day 7 both reporters are observed in the proximal area of the cotyledons as well as

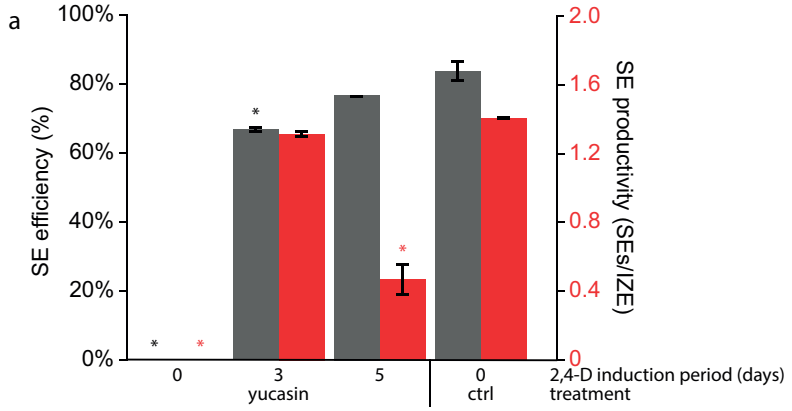

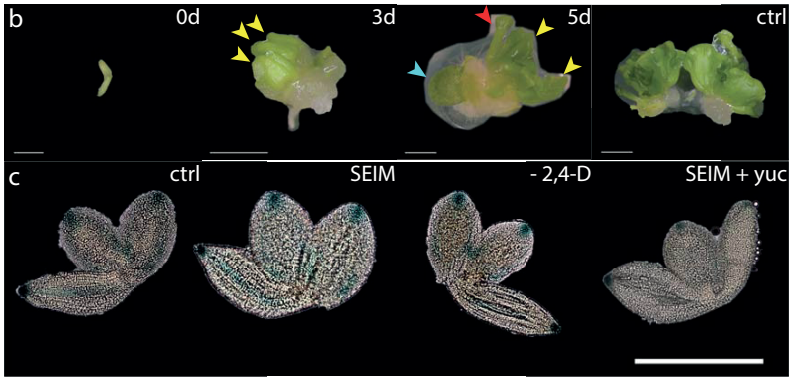

d

	DR5::GUS EXPRESSION				
	TIPS COTYLEDONS		HYPOCOTYL		
	WEAK	STRONG	WEAK	STRONG	*n*
Control	20%	80%	44%	56%	41
SEIM	12%	88%	0%	100%	41
SEIM – 2,4-D	26%	74%	92%	8%	38
SEIM + YUC	78%	22%	89%	11%	27

FIGURE 1 - Effect of yucasin on SE initiation in *Arabidopsis* IZEs.

a) SE efficiency (grey bars) and productivity (red bars) of *Arabidopsis* IZEs cultured on SEIM to which 100µM yucasin was added at the start (0) or at 3 or 5 days after the start of the 14 days incubation period. Control IZEs (0 ctrl) were incubated for 14 days on SEIM without yucasin. Bars represent average values of duplicate experiments with n = 48, error bars indicate SEM. Asterisks denote a significant difference between control and treatment (χ^2-test, $p<0.05$ for SE efficiencies, and Welch *t*-test, $p<0.05$ for SE productivities). b) Representative images of a control IZE (ctrl) or IZEs treated with yucasin after 0, 3 and 5 days of the start of culture. Red arrowheads point at individual somatic embryos, yellow arrowheads point at embryogenic structures, and blue arrowheads indicate shoot-like structures. Scale bar represents 1mm. c) Effect of yucasin on *DR5::GUS* expression in IZEs. Untreated *DR5::GUS* IZEs (ctrl), or *DR5::GUS* IZEs incubated for 4hr on SEIM medium (SEIM), on SEIM without 2,4-D (-2,4-D), or on SEIM supplemented with 100µM yucasin (SEIM + yuc) were stained overnight for GUS activity. Scale bar represents 50µm. Please note that for presentation purposes the original background of the IZE images in b and c was removed. Independent images were placed on a black background. d) IZEs as shown in c were scored for either weak or strong expression in the cotyledon tips and hypocotyl.

the hypocotyl, and expression in the cotyledons tips is only observed in *YUC9*. All four discussed YUCs are strongly expressed on day 7 and weakly or not in prior time points. Therefore we believe that these *YUCs* are most likely involved in somatic embryo development rather than initiation.

A phylogenetic tree of the *Arabidopsis YUCCA* gene family showed that the genes can be grouped into two main clades that are likely to be the result of an early gene duplication event (Figure 2a, Cheng et al., 2007). Interestingly, we noticed that clade members shared expression patterns: e.g. clade 1 *YUCCAs* were either not (*YUC2* and *YUC10*) or only faintly expressed (*YUC4*), or their expression was limited to the vasculature (*YUC6* and *YUC11*) (Figure 2a,b), whereas expression of clade 2 *YUCCAs* was either limited to cotyledon tips (*YUC7, YUC8* and *YUC9*) or was detected in most tissues of the IZE at day 7 (*YUC5*, *YUC8, YUC9*) (Figure 2a,b). This finding corroborates the earlier conclusion by Cheng and coworkers (Cheng, 2006; Cheng et al., 2007) that the sub-functionalization of *YUCCAs* following the early gene duplication that formed the two clades was maintained after subsequent duplication events. Unfortunately, we were not able to study *YUC1* and *YUC3* expression due to malfunctioning of the designed reporter lines.

To correlate *YUC* gene expression patterns with their functionality, we examined available mutant combinations for SE efficiency. It is important to note here that because of our experimental system, our analysis was limited to mutants that developed fertile plants and embryos. Based on the yucasin experiments we expected to see reduced IZE survival, or a slight but significant reduction in SE efficiency (from 80 to 60%). Furthermore, we chose our mutant lines based on a dynamic expression pattern in which expression would increase over time or peak at day 3 or day 5 in regions of SE initiation. This excluded *YUC5* and thus we continued with y*uc8 yuc9* double- and *yuc2 yuc4/+ yuc6* triple loss-of-function mutants that were tested as representatives of respectively clade 1 and clade 2. The *yuc1 yuc10 yuc11* triple loss-of-function mutant was included as negative control, as the corresponding genes were not expressed during IZE-derived SE, or in tissues not directly involved in SE, In addition, the *yuc3* mutant was taken along as part of the *yuc3 yuc9* double mutant, despite the fact that the *YUC3* gene was not included in our expression studies, since it was found to be a target of *BBM* induced SE (Heidman, 2015) and shown to be involved in zygotic embryogenesis (Robert et al., 2013).

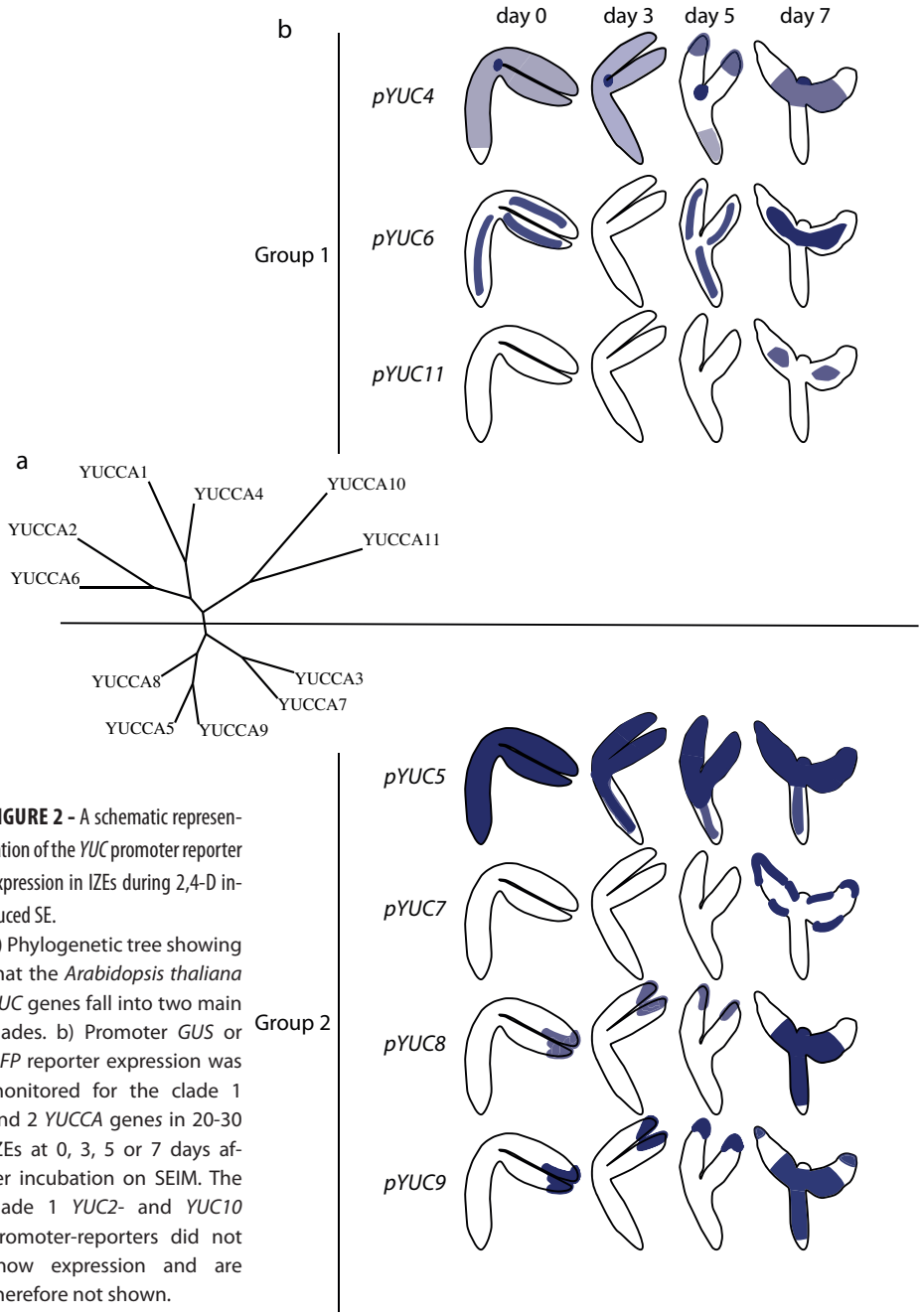

FIGURE 2 - A schematic representation of the *YUC* promoter reporter expression in IZEs during 2,4-D induced SE.
a) Phylogenetic tree showing that the *Arabidopsis thaliana YUC* genes fall into two main clades. b) Promoter *GUS* or *GFP* reporter expression was monitored for the clade 1 and 2 *YUCCA* genes in 20-30 IZEs at 0, 3, 5 or 7 days after incubation on SEIM. The clade 1 *YUC2*- and *YUC10* promoter-reporters did not show expression and are therefore not shown.

For 4 of the 5 tested mutant combinations, including the *yuc1 yuc10 yuc11* negative control, the SE efficiency did not significantly differ from wild type (Figure 3a). Interestingly, however, the *yuc2 yuc4/+ yuc6* triple mutant led to a similar reduction in SE efficiency (81% to 63% SE efficiency) as yucasin treatment, and several mutant IZEs continued with seedling germination programme rather than developing callus or somatic embryos (Figure 3b, blue arrows). As a result, additional shoot or root structures could be found next to somatic embryos on the same explant (Figure 3b). Only few somatic embryos were produced per explant, but if they were present, the somatic embryos exerted a similar phenotype as the wild type.

Previous research on early stage zygotic embryogenesis has shown that *YUCCAs* play a significant role in local auxin biosynthesis that is crucial for embryo development (Cheng, 2006; Cheng et al., 2007; Robert et al., 2013, 2015). Our results confirm this and suggest that at least endogenous auxin production mediated by *YUCCAs* is not needed for SE initiation, but rather for the early survival of IZEs on SEIM and later on for the proper development of individual somatic embryos.

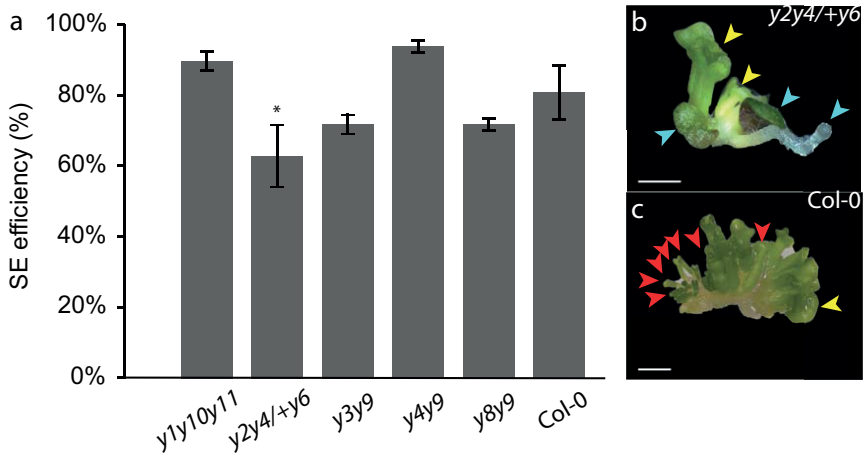

FIGURE 3 - The effect of *yucca* loss-of-function mutations on SE initiation in *Arabidopsis* IZEs.

a) SE efficiency for different *yuc* loss-of-function mutant combinations. Bars represent average values of duplo experiments with n=48 for homozygous lines and n=96 for segregating lines, error bars indicate SEM. Asterisks denote significant differences between wild type (Col-0) and mutant (χ^2-test, $p<0.05$). (b,c) Representative phenotype of the *yuc2 yuc4/+ yuc6* triple mutant (b) and wild-type (Col-0) (c) IZEs following standard SE culture. Red arrowheads point towards individual somatic embryos, yellow arrowheads to embryonic structures and blue arrowheads to shoot structures. Please note that for presentation purposes the original background of the IZE images in b and c was removed and replaced by a black background. Scale bar represents 1mm.

Auxin biosynthesis by TAA1/TAR is required for cell division and proliferation during SE.

Our results indicated that *YUCCAs* are not directly involved in SE initiation. Therefore we set out to investigate whether TAA1/TAR enzymes involved in the Trp → IPyA conversion step have a role during SE initiation. We used the inhibitor L-kynurenine to block the enzymatic activity of TAA1/TAR enzymes. In contrast to the yucasin experiments (Figure 1a), SE efficiency was significantly reduced from 84% in the control treatment to 8%, 3% and 30% for respectively L-kynurenine treatments starting at day 0, 3 and 5 (Figure 4a). Inhibition of the TAA1/TAR enzymes by L-kynurenine resulted in small calli with root and shoot structures, independent of the time point of L-kynurenine application (Figure 4b). In addition, we studied SE initiation by using the embryonic cell fate reporter *pWOX2::NLS-YFP* combined with the auxin response reporter *DR5::RFP* (Chapter 2, Breuninger et al., 2008) during L-kynurenine treatment. IZEs of an *Arabidopsis* line containing both reporters were incubated on SEIM for 3 days and transferred to SEIM with 100µM L-kynurenine or to hormone free medium for 48hr. As a control, a 5 days SEIM culture was included. In the L-kynurenine treated IZEs we did not observe cells marked by *WOX2*, which indicated that SE initiation was completely prohibited. In Chapter 2 we have shown that an elevated auxin response followed by a local minimum is required for SE initiation. This dynamic change was absent in the L-kynurenine treated IZEs. Instead, we observed a reduced expression of *DR5::RFP*, similar to the hormone free treatment (Figure 4c). These results suggested that the Trp → IPyA conversion by TAA1/TARs is essential to SE initiation by enhancing endogenous auxin levels. We noticed that the IZEs treated with L-kynurenine were smaller and hypothesized that this was a result of a defect or reduction in cell division. To investigate this, we performed histological analysis on the base of cotyledons of IZEs that were grown for 5 days on SEIM, and IZEs grown for 3 days on SEIM and subsequently for 2 days on SEIM with 100µM L-kynurenine. In the SEIM cultured IZEs, periclinal and anticlinal symmetric cell divisions were abundantly observed in the (sub)epidermal layer at the base of the cotyledons. Such divisions have been reported to be an indication of SE development (Kurczyńska et al., 2007). In contrast, in the L-kynurenine-treated IZEs the number of cell divisions was limited and most divisions seemed asymmetric (Figure 5b,d). In conclusion, the observed lower auxin response and the disturbed cell divisions producing small calli suggests that *TAA1/TARs*-mediated auxin biosynthesis is triggering an elevated auxin response that is required for appropriate cell division and proliferation during SE initiation.

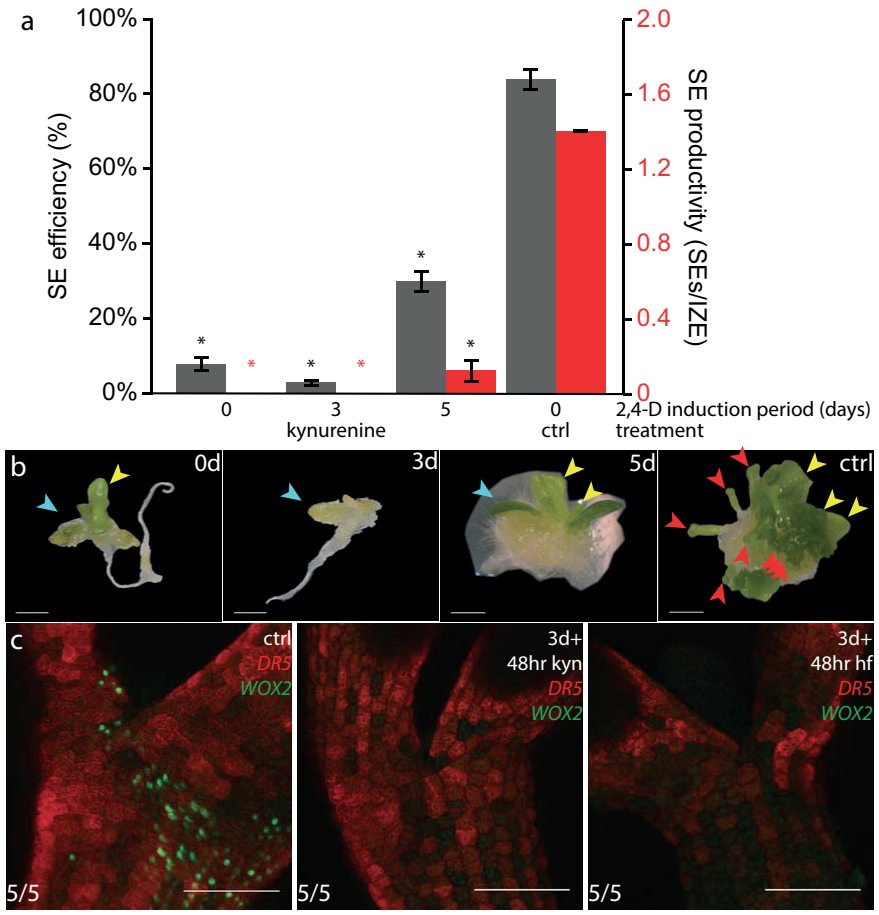

FIGURE 4 - Effect of L-kynurenine on SE initiation in *Arabidopsis* IZEs.

a) SE efficiency (grey bars) and productivity (red bars) of *Arabidopsis* IZEs cultured on SEIM to which 100µM L-kynurenine was added from the start (0) or at 3 or 5 days after the start of incubation. Control IZEs were incubated on SEIM without L-kynurenine (0 ctrl). Bars represent mean values from duplicate experiments with n = 48, error bars indicate SEM. Asterisks denote significant differences between control and treatment. SE efficiencies were compared using the χ^2 test ($p<0.05$), and SE productivities were compared using the Welch *t*-test ($p<0.05$). b) Representative images of phenotype with yucasin treatment after 0, 3 and 5 days and control (ctrl). Red arrowheads point at individual somatic embryos, yellow arrow heads point at embryogenic structures and blue arrow heads indicate shoot-like structures. Please note that for presentation purposes the original background of the IZE images in b and c was removed and replaced by a black background. Scale bar represents 1mm. c) Representative CLSM images of *pWOX2::NLS-YFP* (green) *DR5::RFP* (red) IZEs cultured for 3 days on SEIM followed by 2 days on SEIM in the absence (ctrl) or presence of 100µM L-kynurenine (kyn), or on hormone free (hf) medium. Scale bar represents 50µm.

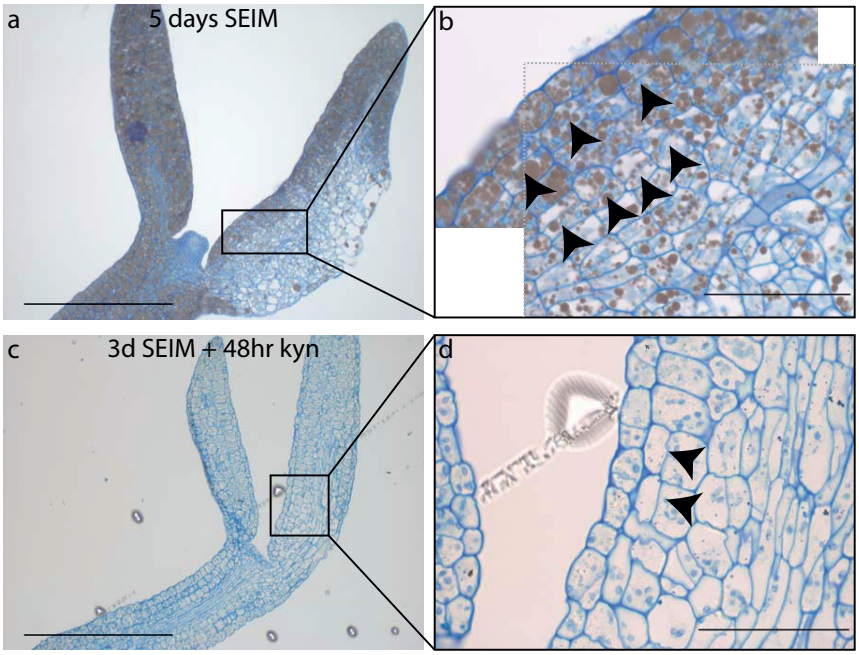

FIGURE 5 - Effect of L-kynurenine treatment on cell divisions in cotyledons of *Arabidopsis* IZEs.
a-b) Representative longitudinal section of an IZE after 5 days SEIM culture (n=5) or c-d) 3days SEIM culture followed by 48hr SEIM culture with 100µM L-kynurenine (n=5). Black arrow heads point at periclinal divisions,. Scale bar in a) and c) represent 250 µm, scale bar in b) and d) represent 50µm. Sections were stained with TBO (blue) for visualizing cells and osmium (brown) was used to color the IZE during embedding and sectioning. Thin sections were made using a microtome at 2µm.

As we observed that L-kynurenine treatment resulted in callus rather than SE development, we investigated whether mutations in the *TAA1/TARs* genes would result in similar phenotypes. To our surprise, however, *wei8-1 tar1-1 tar2-2/+* triple mutant IZEs segregating for the *tar2-2* allele did not show a significant reduction in SE efficiency and productivity compared to wild-type IZEs. We found that the IZEs with the *mp*-like phenotype typical for *wei8-1 tar1-1 tar2-2* homozygous progeny (20 of the 192 IZEs tested) were still able to develop embryogenic calli with somatic embryos similar as wild-type IZEs (Figure 6b, red arrows). We have used a mother plant heterozygous for the *tar2-2* allele, because the availability of IZEs with a *mp*-phenotype was limited. We therefore presumed that the lack of significant differences in phenotype was because at least 75% of IZEs derived from the *wei8-1 tar1-1 tar2-2/+* plant still carried the wild-type *TAR2* allele. We continued with analyzing the auxin response in the triple *wei8-1 tar1-1 tar2-2/+* background to find an explanation for our observations.

Analysis of *DR5::GUS* reporter expression in the triple *wei8-1 tar1-1 tar2-2/+* background showed major differences on day 5 and 7 when SE initiation was expected to occur (Figure 6c,d). Whereas all wild-type IZEs showed a relatively homogeneous *DR5::GUS* expression on both day 5 and day 7 (respectively n=26 and n=31), at day 5 a reduced number of mutant IZEs showed expression in the cotyledons tips (58%), cotyledons base (88%) and root tip (78%) compared to wild-type (respectively 77%, 100%, 85%). On day 7 *DR5::GUS* expression in the mutant IZEs was limited to callus and root tip (Table S3, Figure 6d).

It must be noted that the auxin response restored itself in the root tip at day 7, but was mainly observed in callus that developed in the triple mutant background. As there is still a clear auxin response in the triple mutant, this may explain why *wei8-1 tar1-1 tar2-2/+* did not result in significant differences for SE. The SE initiation still occurs, albeit at a slower rate caused by the reduced auxin response.

In accordance with this slower initiation and development of the somatic embryos, the *wei8-1 tar1-1 tar2-2/+* embryonic calli that developed were smaller (Figure 6d). To confirm this, we scored the frequency of big, small and no calli development after 7 days SEIM culture. In the *DR5::GUS* control 70% of the IZEs developed big calli and only 30% small calli (n=30). In contrast, *wei8-1 tar1-1 tar2-2/+* IZEs developed 31% big calli, 64% small calli and 5% did not develop calli at all (n=59). The lower *DR5* response that was observed together with occurrence of small calli suggests that the *TAA1/TAR*-enhanced auxin response is required for appropriate and efficient cell divisions during SE. Similar cell division defects due to disturbed local auxin homeostasis were also found in embryo and gametophyte development in *Arabidopsis* (Robert et al., 2013; Panoli et al., 2015).

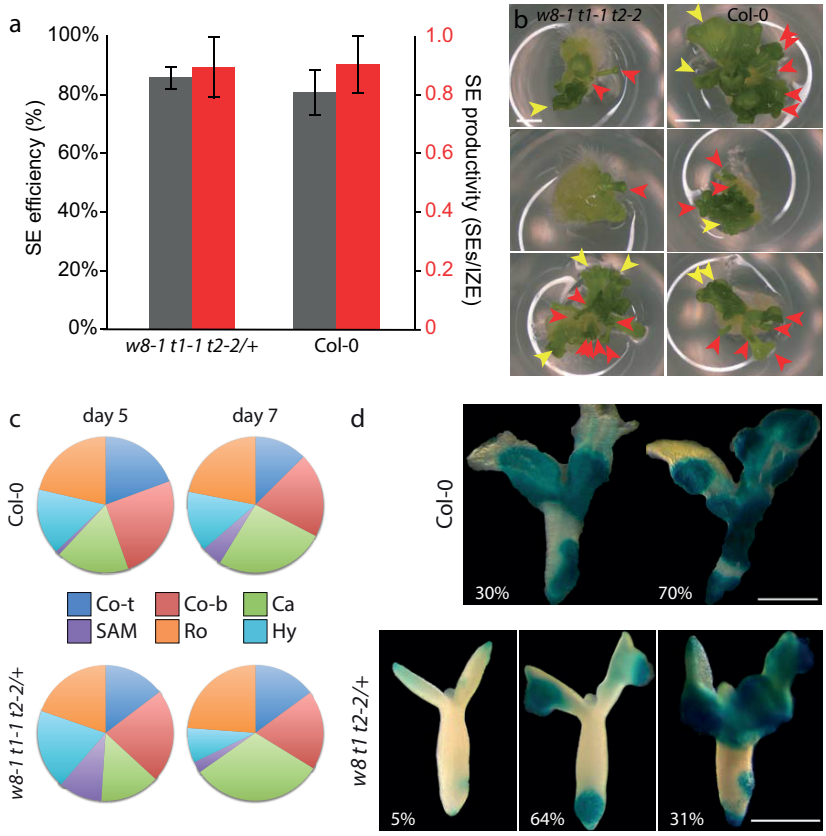

FIGURE 6 - The role of TAA1/TARs during SE initiation in *Arabidopsis* IZEs.
SE efficiency (grey bars) and productivity (red bars) for *wei8-1 tar1-1 tar2-2/+* and Col-0. Bars represent average values of duplicate experiments with n=96, errors bars represent SEM, and asterisks denote significant differences between Col-0 and loss-of-function mutant (χ^2 test, p= 0.05). b) Representative phenotype photos of *wei8-1 tar1-1 tar2-2/+* and Col-0 after standard SE culture. Red arrow heads point towards individual somatic embryos, yellow arrowheads to embryonic structures. Scale bar represents 1mm. c) Graphical representation in pie charts of *DR5::GUS* observations for cotyledon tips (Co-t), cotyledons base (Co-b), callus (Ca), shoot apical meristem (SAM), hypocotyl (Hy) and root (Ro) in Col-0 and *wei8-1 tar1-1 tar2-2/+* after 5 and 7 days standard SEIM culture. d) *DR5::GUS* expression in Col-0 (n=30) and *wei8-1 tar1-1 tar2-2/+* IZE (n=59) after 7 days SEIM culture. Three phenotypic classes were visible after 7 days SEIM culture; IZEs developing big, small or no callus. Percentages denote observations frequencies.

Discussion

The plant hormone auxin controls many aspects of plant development. Many auxin analogs have been made since the 1940s and applied in tissue culture to direct plant regeneration (De Rybel et al., 2009; Simon and Petrášek, 2011; Song, 2014). The synthetic analog 2,4-D is the most abundantly used analog in tissue culture to induce SE. As previous research has shown that 2,4-D causes elevated

levels of auxin (Pasternak, 2002; Michalczuk et al., 1992), we investigated here the role of auxin biosynthesis in SE focusing on two enzymatic steps of the most important Trp dependent pathway, the Trp → IPyA conversion by TAA1/TARs and the IPyA → IAA by YUCCAs.

Using inhibitors for these enzymes we found that the IPyA → IAA conversion has a minor role in SE initiation compared to the Trp → IPyA conversion step. We further demonstrated that most of the *YUCCAs* are not involved in SE initiation, but rather are important during development of the somatic embryo, which is in line with the minor effects of yucasin on SE and a significant reduction in SE productivity on day 5. However, early application of yucasin led to death of IZEs, and the fact that several *YUC* gene candidates have been found to be upregulated in other SE systems (Bai et al., 2013) suggests their importance for the survival of the explants in tissue culture. Besides 2,4-D application, SE can also be induced by ectopic expression of specific transcription factors, such as *LEAFY COTYLEDON1* (*LEC1*), *LEC2, BABYBOOM (BBM)* and *WUSCHEL* (*WUS*) (Lotan et al., 1998; Stone et al., 2001; Boutilier et al., 2002; Zuo et al., 2002). Also in these SE systems, *YUCCA* genes were found to be upregulated. *YUC10* was shown to be upregulated during *LEC1* induced SE (Junker and Bäumlein, 2012; Wójcikowska et al., 2013), whereas *LEC2*- or *BBM*-induced SE led to the upregulation of respectively*YUC1*, *YUC2*, *YUC4*, *YUC10* and *TAA1* (Stone et al., 2008; Wójcikowska et al., 2013) or *YUC3*, *YUC4, YUC8* and *TAA1*) (Heidman, 2015). Thus, an initial rise of auxin mediated by *YUCCAs* in the first 1 to 3 days in SEIM culture seems to be required to maintain embryo viability prior to SE initiation.

However, our results showed that not all *YUCCAs* contribute equally and significantly to SE induction. Firstly, based on our expression analysis we concluded that *YUC2 and YUC11* are not involved during SE initiation and in our SE system, the *yuc2 yuc4/+ yuc6* triple mutant only showed a slight reduction in SE efficiency. This finding is in sharp contrast to a previous study, which reported that *YUCCAs* are essential for SE (Bai et al., 2013). First of all, Bai and co-workers did not test the yucasin inhibitor. Secondly, they detected upregulation of *YUC2* and *YUC11* by qRT-PCR in their system, whereas no expression was observed in our system with GUS reporters. Thirdly, in their hands a *yuc1 yuc2 yuc4 yuc6* quadruple mutant did not show any effect, whereas SE was significantly reduced in a *yuc1 yuc4 yuc10 yuc11* quadruple mutant. In contrast, in our hands only the triple *yuc2 yuc4/+ yuc6* showed a significant effect, whereas the *yuc1 yuc10 yuc11* triple did not. As our *yuc1 yuc10 yuc11* mutant does not include *yuc4* a direct comparison is not possible. More importantly to note is that differences in observations are likely also to be caused by the fact that Bai and coworkers (2013) used a system that studies secondary SE, whereas our system involves the induction of primary

somatic embryos. Both processes may require different auxin mechanisms and can therefore not be compared. What is clear, however, is that YUCCAs act redundantly, and although our data do not completely exclude this redundancy, the yucasin inhibitor results suggest that this pathway is less important for SE initiation. This is in itself a remarkable feature as YUCCAs have been reported to play a key role in zygotic embryogenesis (Cheng, 2006; Stepanova et al., 2007; Robert et al., 2013) and is suggested to be the rate-limiting step of auxin biosynthesis (Zhao, 2014). The auxin biosynthesis is a complicated mechanism and many unknowns remain to be solved such as alternative biosynthesis routes in which YUCCAs may function as well, like the TAM pathway (Ljung, 2013; Mano and Nemoto, 2012; Woodward and Bartel, 2005).

In this chapter we have further shown that SE can be efficiently suppressed by the application of L-kynurenine, a compound that blocks specifically the activity of TAA1/TAR enzymes (He et al., 2011). The dynamic auxin response was absent in L-kynurenine treated IZEs, which corroborates our earlier observation that a dynamic auxin response is required to initiate SE.

However, we found that the loss-of-function mutant *wei8-1 tar1-1 tar2-2/+* did not result in similar phenotypes as the L-kynurenine treatment. One explanation for this is that we cannot measure the effect of the genetic defects because we used a segregating population of the triple mutant and that one functional allele of *TAR2* is sufficient to perform SE similar to wild-type, albeit at slower rate. However, about 20 homozygous triple mutant IZEs could be recognized based on their *mp* phenotype, and these showed somatic embryo development similar to wild-type. To study the functionality of *TAR2*, either more *mp*-like embryos should be studied or its transcriptional as well as translational expression can be studied using reporter lines. In addition, combining reporter assays for *TAA1/TARs* with L-kynurenine treatment would be beneficial to study the specificity of L-kynurenine itself on the TAA1/TAR enzymes during SE initiation. To research the role of TAA1, a new class of TAA1 inhibitors, named "pyruvamines", can be used to perform inhibitor screens (Narukawa-Nara et al., 2016). In addition, other members of the TAA1/TAR family i.e. TAR3 and TAR4 (Tao et al., 2008; Mano and Nemoto, 2012) should also be taken into consideration to fulfill a role in SE initiation. Their role is fairly unknown in plant development thus it would be interesting to use SE to study their function.

We further demonstrated that IZEs in both L-kynurenine and in the *wei8 tar1 tar2/+* knock out developed smaller calli together with a decreased auxin response. This strongly suggests that auxin biosynthesis is required for appropriate cell division during SE, and possibly even for cell wall development, as defects in *WEI8* and *TAR2* have been shown to induce defects in cell wall devel-

opment (Steinwand et al., 2014). It was demonstrated before that defects in cell wall production can lead to callus formation (Nicol et al., 1998; Sato et al., 2001; Ikeuchi et al., 2013; Steinwand et al., 2014). Based on our data it is suggested that auxin biosynthesis is involved during SE initiation in orchestrating cell wall development. Several papers have shown that the auxin biosynthesis-ethylene interaction is of importance to SE and to many other plant development processes (Stepanova et al., 2005; Swarup et al., 2007; Polko et al., 2011; Bai et al., 2013; Nowak et al., 2014). During SE initiation, ethylene levels are decreased and mutations in ethylene signaling or treatment with precursors of ethylene disrupts SE initiation and activate auxin biosynthesis (Jiménez, 2005; Bai et al., 2013; Nowak et al., 2014). *YUC1* and *YUC4* expression is reduced in embryogenic calli treated with the ethylene precursor ACC (Bai et al., 2013). Similarly, *LEC2* activates auxin biosynthesis through *YUCCAs* simultaneous causing ethylene biosynthesis to be inhibited (Wójcikowska et al., 2013). Moreover, a knockout of *ETHYLENE RESPONSE FACTOR022 (ERF022)* has reduced *YUC1* and *YUC4* expression levels during SE (Nowak et al., 2014). Ethylene can regulate organ development by either directly regulating local auxin biosynthesis through *WEI2/WEI7* or indirectly through a signaling pathway, activating auxin transport and biosynthesis (Ruzicka et al., 2007; Stepanova et al., 2008; Li et al., 2006). A detailed analysis of the dynamic auxin response with ethylene application and its inhibitors for biosynthesis aminoethoxyvinylglycine (AVG) (Strader et al., 2010), for signaling silver thiosulfate (STS) (McDaniel and Binder, 2012) and 1-methylcyclopropene (1-MCP) (Hall et al., 2000) would contribute to a more in depth understanding of the auxin biosynthesis – ethylene relationship during SE initiation.

Methods

Plant lines

All *Arabidopsis thaliana* lines described below are in Columbia wild-type (Col-0) background. The *pWOX2::NLS-YFP* line was kindly donated by Thomas Laux and is resistant to phosphinothricin (ppt) (Breuninger et al., 2008). The *DR5::RFP* line was donated by Eva Benkova and is resistant to hygromycin (hyg) (Marhavý et al., 2011). The *yuc1 yuc10 yuc11* and *yuc2 yuc4/+ yuc6* triple mutants were obtained from the original *yuc1 yuc4/+ yuc10 yuc11* and *yuc1/+ yuc2 yuc4/+ yuc6* lines kindly donated by Yunde Zhao (Cheng, 2006; Cheng et al., 2007).

The *YUC2/5/6/7/8/9/10/11* promoter-*GFP-GUS* or *YUC1/4* promoter *NLS-3xGFP* reporter fusion lines are kanamycine (kan) resistant and together with the *yuc3 yuc9* and *yuc4 yuc9* double mutants they were kindly provided by Helene

Robert-Boisivon. The mutant lines *yuc3* (GK-376G12, part of set 436084), *yuc4* (Cheng et al. (2006) and *yuc9* (sail_871_G01) (Robert et al., 2013), *yuc8* (N655757/ SALK_096110C), *yuc9* (sail_871_G01) and *wei8-1 tar1-1 tar2-2/+ DR5::GUS* (N16420/ CS16420) were ordered from NASC.

Genotyping

Sequences of DNA primers used for genotyping are provided in Table S1. All PCR reactions were performed using DreamTaq DNA polymerase (ThermoFisher Scientific, EP0705) on genomic DNA isolated as described by Giraudat (2003), melting temperature and annealing time respectively was 55°C and 60s, unless otherwise stated.

Plant tissue culture and growth conditions

Arabidopsis seeds were surface sterilized and germinated on MA medium (Masson and Paszkowski, 1992) complemented with 1% (w:v) sucrose, and 0.8% (w:v) Daishin agar, pH5.8. For antibiotic selection ppt, hyg or kan was added to the medium after autoclaving at a final concentration of 20mg/mL for ppt and hyg, and of 50mg/mL for kan. Seven to ten days after germination (dag), seedlings were transferred to a mixture of soil and sand, 2 per pot, and grown under a 16hr photoperiod and 70% relative humidity. IZEs were harvested from plants 1-2 weeks after flowering. The siliques were surface sterilized with a 20% bleach/ 70% ethanol solution for 5min. and rinsed at least three times with sterile water. SE-inducing medium (SEIM) consisted of B5 medium, with 4.5µM 2,4-D, 2% (w:v) sucrose and 0.8% (w:v) Daishin agar (Gaj, 2011; Nowak et al., 2012). Hormone free medium was MA medium (Masson and Paszkowski, 1992). Media were sterilized by autoclaving at 120°C for 20min SE induction was performed in sterile 48-wells plates (Greiner cellstar art. nr. 677180) that were filled with 400µL SEIM or hormone free medium using a repeater pipet. IZEs were placed on SEIM (one per well) and incubated overnight at 4°C in the dark followed by incubation at 21°C and under a 16hr photoperiod for a standard period of 14 days, followed by 7 days incubation on hormone free medium (standard SE culture). Yucasin (5-(4-Chlorophenyl)-2,4-dihydro-[1,2,4]-triazole-3-thione, CAS 26028-65-9, Sigma 573769) and L-Kynurenine (Sigma k8625, CAS 2922-83-0) were ordered from Sigma and were added to SEIM from a 50mM stock solution in DMSO to a final concentration of 100µM.

For the SE efficiency studies with inhibitors or mutant IZEs, IZEs synchronized in their developmental stage were obtained by manual pollination. For this purpose, the 2 or 3 oldest but still closed flower buds of primary inflorescence stems were emasculated and pollinated and 12 days after pollination (dap) IZEs were

excised from the ovule using a dissecting microscope. Per two parent plants, 2-3 sets of 2-3 closed flower buds were emasculated.

To keep data comparable between inhibitor experiments, large-scale experiments were set up as follows: the 100µM yucasin, 100µM L-kynurenine and 2,4-D control treatments were performed in duplicate for all 2,4-D pre-induction periods (0, 3 and 5 days). Per treatment, 48 IZEs were used, one IZE per well in a 48-wells plate. For the 3 and 5 days induction, a large pool of IZEs was cultured in multiple 48-wells plates. At day 3 and day 5 48 IZEs were selected randomly out of the different plates for each treatment and transferred to plates containing 2,4-D and 100µM inhibitor. For the day 0 treatment 4 siliques were used to compile 1 plate per treatment (12 IZEs per silique).

The mutant studies were performed by culturing 48 IZEs per genotype in duplicates.

For confocal or light microscopy analysis non-synchronized late IZEs from more or less the same developmental stage were selected based on their size as described by (Gaj, 2011). Broken or damaged IZEs were discarded and not used.

Statistics of SE

To quantify SE, four categories were used to score 1) embryogenic tissue (also referred to as embryogenic callus), if no individual somatic embryos were found but embryogenic tissue developed. Embryogenic tissue was defined as smooth green structures without trichomes, that either looked like fused cotyledons or like fused zygotic embryos 2) SE forming IZEs, if individual somatic embryos were observed that were attached to the IZE by their root pole. In that case, the number of individual somatic embryos was counted. 3) Non-embryogenic callus forming IZEs, if callus was formed that remained white-yellowish without developing somatic embryos or embryogenic tissue 4) Dead IZEs, if the tissue turned white, showed no growth and maintained their original size.

Category 1 and 2 were merged to quantify the number of responding IZEs that produced embryogenic tissue. The SE efficiency was then calculated as (Luo and Koop, 1997)

$$SE\ efficiency = \frac{N_r}{N_t} \quad 100\%$$

N_r = the number of responding explants. N_t = total number of explants tested.

SE productivity was calculated as

$$SE\ productivity = \frac{N_i}{N_t}$$

N_i = the number of individual somatic embryos observed. N_t = the total number of IZEs that were tested (including the ones that died).

Statistics for SE efficiency were performed in Microsoft Excel, using the χ^2-test for association (Holmes et al., 2011). For SE productivity, a Welch *t*-test was performed in Rstudio (Pace, 2015).
For inhibitor studies we compared the control treatments to check whether refreshment of SEIM would contribute to SE efficiency and productivity. The two controls were not statistically different for SE efficiency and productivity (respectively χ^2_{calc}=2.9, and *t*-test p-value 0.524, described in Chapter 2) and for this reason we performed all statistical tests between the treatment and the 0 days control.

GUS staining

Staining for B-glucuronidase (GUS) activity was performed as described by Malamy and Benfey (1997) with the following modifications: The staining solution was made as follows: a K/NaPI buffer was made by adding approximately 50mL 0.5M KH_2PO_4 to 125mL 0.5M Na_2HPO_4 tuntil pH reached 7.0.40mL of this solution was diluted with MilliQ to 200mL, and.subsequently2mL 1M EDTA (pH8.0), 2mL 0.1M $K_4Fe(CN)_6$, 2mL 0.1M ($K_3Fe(CN)_6$ and 200uL 0.1% Triton were added. X-gluc (Duchefa, X1402) was pre-dissolved in DMSO at 100mg/mL and was added to the staining solution at a final concentration of 1mg/mL. The bottle with the solution was wrapped in aluminium foil and stored at 4°C for a maximum of 6 months. Samples were submerged in 1-2mL staining solution and incubated for 3hr at 37°C followed by overnight incubation at room temperature to increase staining. Samples were destained with 0.24M HCL 20% methanol for 15min at 55°C, followed by 15min incubation in 7% (w:v) natriumhydroxide/ 60% ethanol for clearing. Samples were rehydrated through an ethanol series 50% - 30% - 10% - 5%, with 5min incubation between each step. To completely remove chlorophyll from the embryos, samples were then cleared for at least 1hr with a 25% (w:v) chloralhydrate in 50% glycerol solution.
Images were taken with a stereomicroscope Leica DC 500 using the Leica Application Suite v2.8.1 software or a DIC/Nomarski AxioCam using AxioVision40 V4.7.2.0 software and a 10x objective. Image editing was performed with FIJI and Adobe Photoshop CS5.1 and figures were assembled in Adobe Illustrator CS5.1.

Histology

To make thin longitudinal sections of IZEs, samples were fixated overnight at 4°C in 2% (w:v) paraformaldehyde/ 2.5% (v:v) gluteraldehyde/ 1x phosphate buffered saline (PBS, pH7.4, 8g NaCl, 0.2g KCl, 1.44g Na_2HPO_4, 0.24g KH_2PO_4 per liter) and colored with osmium for a few seconds for visibility during the embedding process. Samples were washed twice in PBS for 15min. Samples were then dehydrated through an ethanol serie 70% - 80% - 90% - 96% - 100% for at least one hour per step. Subsequently, samples were incubated twice in propylene oxide for 15min and in a 1:1 propylene:EPON mixture for 2hr at room temperature. The remaining propylene oxide: EPON mix was then added to the samples and left overnight. Samples were embedded by filling up molds with EPON and carefully placing the samples into the molds with the root pointing downwards and cotyledons upwards in the same x,y plane. Samples were then left to dry overnight at 60°C. The EPON embedded samples were cut longitudinal, at 2µm using a microtome and glass knives. The slices were then stained with 1% (w:v) Toluidine Blue O/1% (w:v) borax for 20-25s and covered in a thin layer of EPON with a cover glass on an object glass. Slides were left overnight at 60°C to dry. Photos were taken with a DIC/Nomarski ZEISS AxioCam using AxioVision40 V4.7.2.0 software and a 20x and 100x objective. Image editing was performed with FIJI and Adobe Photoshop CS5.1 and figures were assembled in Adobe Illustrator CS5.1.

Microscopy

Images of (GUS stained) IZEs were taken with Leica DC 500 stereomicroscope using the Leica Application Suite v2.8.1 software or a Zeiss Axioplan DIC/Nomarski microscope equipped with Axiocam MRc5 camera and AxioVision40 V4.7.2.0 software and a 10x objective. Image editing was performed in FIJI and Adobe Photoshop CS5.1 and figures were assembled in Adobe Illustrator CS5.1

Confocal Laser Scanning Microscopy (CSLM) was performed with a ZEISS LSM510 exciter equipped with argon and helium/neon lasers. GFP and YFP were detected using a 488nm band pass filter for excitation and a 500-530nm band pass filter for emission. Simultaneously, chlorophyll background fluorescence was captured with a 650nm long pass emission filter. RFP was excited at 530nm and was captured with a 550-600nm band pass emission filter. Images were captured with ZEISS ZEN2009 software.

Samples were prepared on a microscope slide by embedding IZEs in a thin layer of 0.5% low melting point agarose, and adding a droplet of water before covering with a cover slip.

Construction of phylogenetic tree

Genomic sequences for *YUCCAs* were obtained from the TAIR database (www.arabidopsis.org, visited 2015) and a radial phenogram was constructed using www.phylogeny.fr (Dereeper et al., 2008, 2010; Edgar, 2004; Castresana, 2000; Guindon and Gascuel, 2003; Anisimova and Gascuel, 2006; Chevenet et al., 2006, visited 2015).

Acknowledgements

C.P. was supported by an NWO-TTI-Green Genetics core project grant (NWO 828.11.004) to R.O. from the Earth and Life Sciences Division with financial support from the Netherlands Organisation for Scientific Research (NWO). We thank Gerda Lamers for her help with microscopy.

Supplemental information

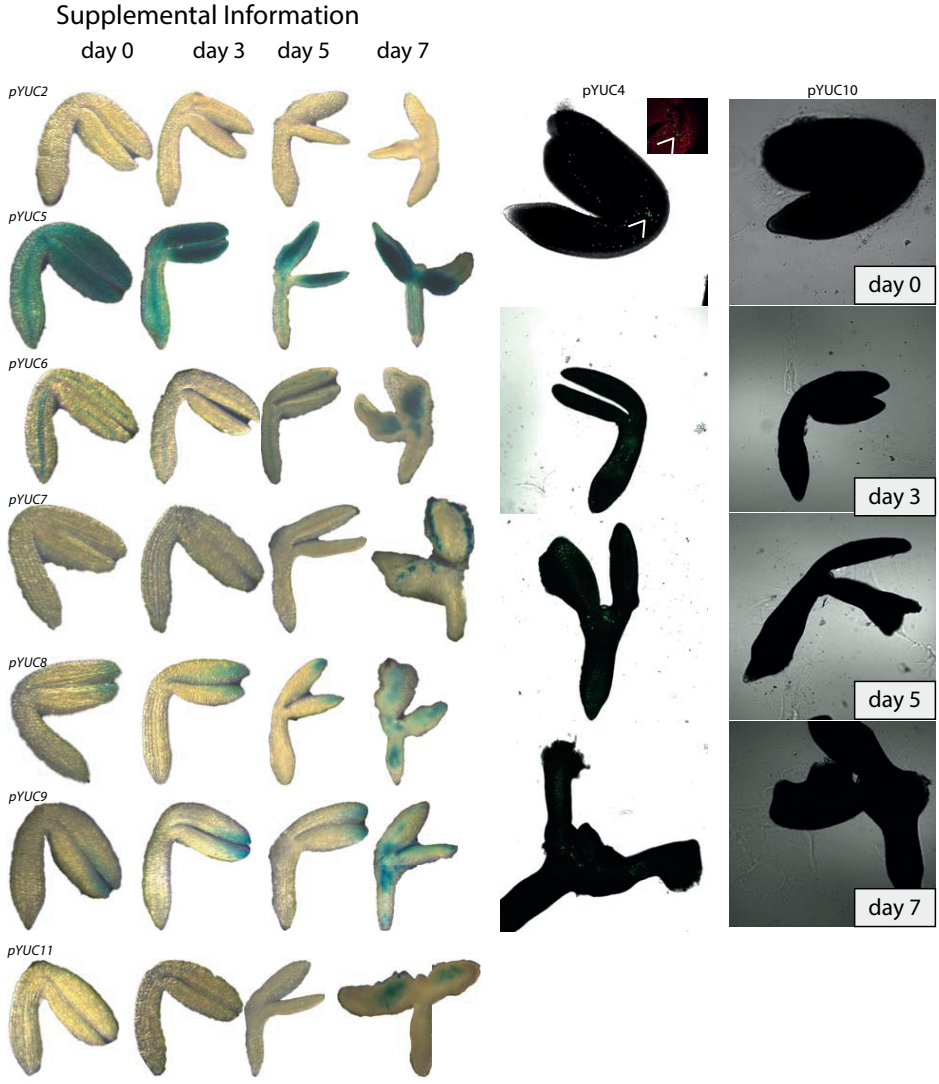

FIGURE S1 - *YUC* promoter expression in IZEs during 2,4-D induced SE. Representative images of GUS or GFP driven by *YUC* promoters in *Arabidopsis* IZEs on day 0, day 3, day 5 and day 7. The white arrowhead marks the shoot apical meristem.

TABLE S1 - *YUC* promoter expression in IZEs during 2,4-D induced SE. Observation frequencies of GUS or GFP driven by *pYUCx* promoters in *Arabidopsis* IZEs on day 0, day 3, day 5 and day 7.

		DAY 0	DAY 3	DAY 5	DAY 7			DAY 0	DAY 3	DAY 5	DAY 7
pYUC2	Cotyledon	4	0	0	0	**pYUC5**	Cotyledon	100	100	100	100
	SAM	0	0	0	0		SAM	100	100	100	100
	Hypocotyl	0	0	0	0		Hypocotyl	100	100	100	100
	Root	0	0	0	0		Root	100	100	100	100
	Callus	0	0	0	0		Callus	0	0	100	100
	n	28	28	28	32		n	34	34	34	34
pYUC4	Cotyledon	100	50	20	40	**pYUC7**	Cotyledon	0	0	0	89
	SAM	100	80	50	80		SAM	0	0	0	6
	Hypocotyl	100	60	10	0		Hypocotyl	0	0	0	6
	Root	0	0	0	0		Root	0	0	0	0
	Callus	0	0	0	80		Callus	0	0	0	83
	n	10	10	10	10		n	27	27	29	35
pYUC6	Cotyledon	29	43	76	100	**pYUC8**	Cotyledon	55	88	100	97
	SAM	0	0	14	100		SAM	0	0	12	79
	Hypocotyl	29	96	76	100		Hypocotyl	0	0	0	76
	Root	29	22	57	27		Root	0	0	0	31
	Callus	0	0	0	100		Callus	0	0	0	97
	n	28	23	37	22		n	31	17	17	29
pYUC10	Cotyledon	0	0	0	0	**pYUC9**	Cotyledon	46	100	96	90
	SAM	0	0	0	0		SAM	0	0	7	25
	Hypocotyl	0	0	0	0		Hypocotyl	0	0	4	60
	Root	0	0	0	0		Root	0	0	21	10
	Callus	0	0	0	0		Callus	0	0	0	45
	n	10	10	10	9		n	24	19	28	20
pYUC11	Cotyledon	0	0	0	56						
	SAM	0	0	0	0						
	Hypocotyl	0	0	0	0						
	Root	0	0	0	0						
	Callus	0	0	0	81						
	n	18	11	26	27						

TABLE S2 - Frequency table for Figure 6e. *DR5::GUS* observations for cotyledon tips (Co-t), cotyledons base (Co-b), callus (Ca), shoot apical meristem (SAM), hypocotyl (Hy) and root (Ro) in Col-0 and *wei8-1 tar1-1 tar2-2/+* after 5 and 7 days standard SEIM culture.

	D5		D7	
Co-t	77%	58%	48%	45%
Co-b	100%	88%	77%	57%
Ca	69%	56%	100%	95%
SAM	4%	41%	19%	8%
Hy	62%	75%	55%	25%
Ro	85%	78%	84%	72%
n	26	64	31	60

TABLE S3 - Plant lines used, with their origin and selection method

PLANT LINE	ORIGIN	SELECTION	ADDITIONAL INFORMATION
pWOX2::NLS:YFP	Breuninger et al. 2008	ppt	
DR5::RFP	Eva Benkova	hyg	
yuc1 yuc10 yuc11	Cheng et al. 2006,2007	PCR	
yuc2 yuc4 yuc6	Cheng et al. 2006,2007	PCR	
yuc3 yuc9	Robert et al. 2013	PCR	yuc3 (GK-376G12, part of set 436084) yuc9 (sail_871_G01)
yuc4 yuc9	Robert et al. 2013	PCR	*yuc4* from Cheng et al. (2006) yuc9 (sail_871_G01)
yuc8	SALK	PCR	N655757/SALK_096110C
yuc9	SALK	PCR	sail_871_G01
wei8-1 tar1-1 tar2-2/+ DR5::GUS	SALK	PCR	N16420/ CS1642
YUC2p:eGFP-GUS	Robert, H.	kan	T3.303.2
YUC4p:3xnGFP	Robert, H.	kan	T4.25W-3.3.1
YUC5p:eGFP-GUS	Robert, H.	kan	T3.104.5
YUC6p:eGFP-GUS	Robert, H.	kan	T3.401.2
YUC7p:eGFP-GUS	Robert, H.	kan	T3.405.5
YUC8p:eGFP-GUS	Robert, H.	kan	T3.204.1
YUC9p:eGFP-GUS	Robert, H.	kan	T3.203.1
YUC10p:3xnGFP	Robert, H.	kan	T4-2.1.1.2
YUC11p:eGFP-GUS	Robert, H.	kan	T3.301.1

TABLE S4 - Primer sequences for genotyping. GSP is gene specific primer, BP is border specific primer. All reactions were carried out with genomic DNA, DreamTaq polymerase, melting temperature = 55ºC, annealing time = 60s, unless otherwise stated.

GENE	PRIMER ORIENTATION	SEQUENCE (5′ - 3′)	REMARKS
yuc1	GSP left	GGTTCATGTGTTGCCAAGGGA	Tm = 61C
	GSP right	CCTGAAGCCAAGTAGGCACGTT	
	Border	LBB1.3 salk	
yuc2	GSP left	CTGCATACAATCCGCTTTCGC	
	GSP right	TTCTTGCATTTTCTCGCTCTACG	
	Border	LBB1.3 salk	
yuc3	GSP left	ATATTGACCATCATACTCATTGC	
	GSP right	TTATAGCCCCTAAAACAGAGCATC	
yuc4	GSP left	CCCTTCTTAGACCTACTCTAC	
	GSP right	GCCCAACGTAGAATTAGCAAG	
	Border	TACGAATAAGAGCGTCCATTTTAGAGTGA	
yuc6	GSP left	CCAGCCTTTGTATTTTCCCGT	
	GSP right	CCGGAAAAAGGGTTCTTGTCG	
	Border	LBB1.3 salk	
yuc8	GSP left	GACTCACTCTTCGACACGGTC	
	GSP right	GAACCGGGTAGCGTAAGACTC	
	Border	LBB1.3 salk	
yuc9	GSP left	TTAAGCAACTGAGATGCATC	Tm = 55C, At = 45s
	GSP right	TAGCATCTGAATTTCATAACCAATCTCGATACAC	
	Border	LB1 sail	
yuc10	GSP left	CCTGAATCTCGCCATCGCGAATC	
	GSP right	CCAAAGAGCTTTTCGTCAACTACC	
	Border	CGTGTGCCAGGTGCCCACGGAATAGT	
yuc11	GSP left	TGTCAACTCCCTCACATGCCA	
	GSP right	CAGATCTCCATCATCGACCTGTGT	
	Border	JMLB1	
wei8-1	GSP left	CATCAGAGAGACGGTGGTGAAC	
	GSP right	GCTTTTAATGAGCTTCATGTTGG	
	Border	DWLB1	
tar1-1	GSP left	CACCATGATGGTTGGGTGTGAAAACTC	
	GSP right	AGGCTCGACGCATTTGAGATC	
	Border	DWLB1	
tar2-2	GSP left	GCACGCAAGTGAAGCTCCAAGC	
	GSP right	ATACTGTGGCCAATAGTAAGCC	
	Border	JMLB1	

LB1 sail	GCCTTTTCAGAAATGGATAAATAGCCTTGCTTCC
LBB1.3 salk	ATTTTGCCGATTTCGGAAC
JMLB1	GGCAATCAGCTGTTGCCCGTCTCACTGGTG
DWLB1	CATACTCATTGCTGATCCATGTAGATTTCC

References

Anisimova, M. and Gascuel, O. (2006). Approximate likelihood-ratio test for branches: a fast, accurate, and powerful alternative. Syst. Biol. **55**: 539–552.

Bai, B., Su, Y.H., Yuan, J., and Zhang, X.S. (2013). Induction of somatic embryos in *Arabidopsis* requires local *YUCCA* expression mediated by the downregulation of ethylene biosynthesis. Mol. Plant **6**: 1247–1260.

Boutilier, K., Offringa, R., Sharma, V.K., Kieft, H., Ouellet, T., Zhang, L., Hattori, J., Liu, C., van Lammeren, A.A.M., Miki, B.L.A., Custers, J.B.M., and van Lookeren Campagne, M.M. (2002). Ectopic expression of *BABY BOOM* triggers a conversion from vegetative to embryonic growth. Plant Cell **14**: 1737–1749.

Breuninger, H., Rikirsch, E., Hermann, M., Ueda, M., and Laux, T. (2008). Differential expression of *WOX* Genes mediates apical-basal axis formation in the *Arabidopsis* embryo. Dev. Cell **14**: 867–876.

Castresana, J. (2000). Selection of conserved blocks from multiple alignments for their use in phylogenetic analysis. Mol. Biol. Evol. **17**: 540–552.

Cheng, Y. (2006). Auxin biosynthesis by the *YUCCA* flavin monooxygenases controls the formation of floral organs and vascular tissues in *Arabidopsis*. Genes Dev. **20**: 1790–1799.

Cheng, Y., Dai, X., and Zhao, Y. (2007). Auxin synthesized by the *YUCCA* flavin monooxygenases is essential for embryogenesis and leaf formation in *Arabidopsis*. Plant Cell **19**: 2430–2439.

Chevenet, F., Brun, C., Bañuls, A.-L., Jacq, B., and Christen, R. (2006). TreeDyn: towards dynamic graphics and annotations for analyses of trees. BMC Bioinformatics **7**: 439.

Dereeper, A., Audic, S., Claverie, J.-M., and Blanc, G. (2010). BLAST-EXPLORER helps you building datasets for phylogenetic analysis. BMC Evol. Biol. **10**: 8.

Dereeper, A., Guignon, V., Blanc, G., Audic, S., Buffet, S., Chevenet, F., Dufayard, J.-F., Guindon, S., Lefort, V., Lescot, M., Claverie, J.-M., and Gascuel, O. (2008). Phylogeny.fr: robust phylogenetic analysis for the non-specialist. Nucleic Acids Res. **36**: W465–W469.

Edgar, R.C. (2004). MUSCLE: multiple sequence alignment with high accuracy and high throughput. Nucleic Acids Res. **32**: 1792–1807.

Friml, J., Vieten, A., Sauer, M., Weijers, D., Schwarz, H., Hamann, T., Offringa, R., and Jürgens, G. (2003). Efflux-dependent auxin gradients establish the apical-basal axis of *Arabidopsis*. Nature **426**: 147–153.

Gaj, M.D. (2001). Direct somatic embryogenesis as a rapid and efficient system for in vitro regeneration of *Arabidopsis thaliana*. Plant Cell. Tissue Organ Cult. **64**: 39–46.

Gaj, M.D. (2011). Somatic embryogenesis and plant regeneration in the culture of *Arabidopsis* thaliana (L.) Heynh. immature zygotic embryos. Methods **710**: 257–265.

Giraudat, J. (2003). Practical course on genetic and molecular analysis of *Arabidopsis*. In EMBO course, J. Giraudat, ed (EMBO), pp. 1–21.

Guindon, S. and Gascuel, O. (2003). A simple, fast, and accurate algorithm to estimate large phylogenies by maximum likelihood. Syst. Biol. **52**: 696–704.

Hall, A.E., Findell, J.L., Schaller, G.E., Sisler, E.C., and Bleecker, A.B. (2000). Ethylene perception by the ERS1 protein in *Arabidopsis*. Plant Physiol. **123**: 1449–1458.

He, W., Brumos, J., Li, H., Ji, Y., Ke, M., Gong, X., Zeng, Q., Li, W., Zhang, X., An F., Wen, X., Li, P., Chu, J., Sun, X., Yan, C., Yan, N., Xie, D-D., Raikhel, N., Yang, Z., Stepanova, A., Alonso, J.M., and Guo H. (2011). A small-molecule screen identifies L-kynurenine as a competitive

inhibitor of TAA1/TAR activity in ethylene-directed auxin biosynthesis and root growth in *Arabidopsis*. Plant Cell **23**: 3944–3960.

Heidman, I. (2015). Applied and fundamental aspects of *BABY BOOM*-mediated regeneration. Thesis, Wageningen Univ.

Holmes, D., Moody, P., and Dine, D. (2011). Research methods for biosciences 2nd ed. O. university Press, ed (Oxford University Press).

Ikeuchi, M., Sugimoto, K., and Iwase, A. (2013). Plant callus: mechanisms of induction and repression. Plant Cell **25**: 3159–3173.

Jiménez, V.M. (2005). Involvement of Plant Hormones and Plant Growth Regulators on in vitro somatic embryogenesis. Plant Growth Regul. **47**: 91–110.

Junker, A. and Bäumlein, H. (2012). Multifunctionality of the *LEC1* transcription factor during plant development. Plant Signal. Behav. **7**: 1718–1720.

Korasick, D. A., Enders, T. A., and Strader, L.C. (2013). Auxin biosynthesis and storage forms. J. Exp. Bot. **64**: 2541–2555.

Kurczyńska, E.U., Gaj, M.D., Ujczak, A., and Mazur, E. (2007). Histological analysis of direct somatic embryogenesis in *Arabidopsis thaliana* (L.) Heynh. Planta **226**: 619–628.

Li, J., Dai, X., and Zhao, Y. (2006). A role for *AUXIN RESPONSE FACTOR19* in auxin and ethylene signaling in *Arabidopsis*. Plant Physiol. **140**: 899–908.

Ljung, K. (2013). Auxin metabolism and homeostasis during plant development. Development **140**: 943–950.

Lotan, T., Ohto, M., Yee, K.M., West, M. A., Lo, R., Kwong, R.W., Yamagishi, K., Fischer, R.L., Goldberg, R.B., and Harada, J.J. (1998). *Arabidopsis LEAFY COTYLEDON1* is sufficient to induce embryo development in vegetative cells. Cell **93**: 1195–1205.

Luo, Y. and Koop, H.U. (1997). Somatic embryogenesis in cultured immature zygotic embryos and leaf protoplasts of *Arabidopsis thaliana* ecotypes. Planta **202**: 387–396.

Malamy, J.E. and Benfey, P.N. (1997). Organization and cell differentiation in lateral roots of *Arabidopsis thaliana*. Development **124**: 33–44.

Marhavý, P., Bielach, A., Abas, L., Abuzeineh, A., Duclercq, J., Tanaka, H., Pařezová, M., Petrášek, J., Friml, J., Kleine-Vehn, J., and Benková, E. (2011). Cytokinin modulates endocytic trafficking of PIN1 auxin efflux carrier to control plant organogenesis. Dev. Cell **21**: 796–804.

Mano, Y. and Nemoto, K. (2012). The pathway of auxin biosynthesis in plants. J. Exp. Bot. 63: 2853–2872.

McDaniel, B.K. and Binder, B.M. (2012). *ETHYLENE RECEPTOR1* (*ETR1*) is sufficient and has the predominant role in mediating inhibition of ethylene responses by silver in *Arabidopsis thaliana*. J. Biol. Chem. **287**: 26094–26103.

Michalczuk, L., Ribnicky, D.M., Cooke, T.J., and Cohen, J.D. (1992). Regulation of indole-3-acetic acid biosynthetic pathways in carrot cell cultures. Plant Physiol. **100**: 1346–1353.

Nicol, F., His, I., Jauneau, A., Vernhettes, S., Canut, H., and Höfte, H. (1998). A plasma membrane-bound putative endo-1,4-β-D-glucanase is required for normal wall assembly and cell elongation in *Arabidopsis*. EMBO J. **17**: 5563–5576.

Nishimura, T., Hayashi, K.-I., Suzuki, H., Gyohda, A., Takaoka, C., Sakaguchi, Y., Matsumoto, S., Kasahara, H., Sakai, T., Kato, J.-I., Kamiya, Y., and Koshiba, T. (2014). Yucasin is a potent inhibitor of YUCCA, a key enzyme in auxin biosynthesis. Plant J. **77**: 352–66.

Nowak, K., Wójcikowska, B., and Gaj, M.D. (2014). *ERF022* impacts the induction of somatic embryogenesis in *Arabidopsis* through the ethylene-related pathway. Planta **241**: 967–985.

Nowak, K., Wojcikowska, B., Szyrajew, K., and Gaj, M.D. (2012). Evaluation of different embryogenic systems for production of true somatic embryos in *Arabidopsis*. Biol. Plant. **56**: 401–408.

Pace, L. (2015). Beginning R: an introduction to statistical programming (Apress).

Panoli, A., Martin, M.V., Alandete-Saez, M., Simon, M., Neff, C., Swarup, R., Bellido, A., Yuan, L., Pagnussat, G.C., and Sundaresan, V. (2015). Auxin import and local auxin biosynthesis are required for mitotic divisions, cell expansion and cell specification during female gametophyte development in *Arabidopsis thaliana*. PLoS One **10**: e0126164.

Pasternak, T.P. (2002). The role of auxin, pH, and stress in the activation of embryogenic cell division in leaf protoplast-derived cells of alfalfa. Plant Physiol. **129**: 1807–1819.

Polko, J.K., Voesenek, L.A.C.J., Peeters, A.J.M., and Pierik, R. (2011). Petiole hyponasty: an ethylene-driven, adaptive response to changes in the environment. AoB Plants **2011**: plr031–plr031.

Raghavan, V. (2004). Role of 2,4-dichlorophenoxyacetic acid (2,4-D) in somatic embryogenesis on cultured zygotic embryos of *Arabidopsis*: cell expansion, cell cycling, and morphogenesis during continuous exposure of embryos to 2,4-D. Am. J. Bot. **91**: 1743–1756.

Reinhardt, D., Pesce, E.-R., Stieger, P., Mandel, T., Baltensperger, K., Bennett, M., Traas, J., Friml, J., and Kuhlemeier, C. (2003). Regulation of phyllotaxis by polar auxin transport. Nature **426**: 255–260.

Robert, H.S., Crhak Khaitova, L., Mroue, S., and Benkova, E. (2015). The importance of localized auxin production for morphogenesis of reproductive organs and embryos in *Arabidopsis*. J. Exp. Bot. **66**: 5029–5042.

Robert, H.S., Grones, P., Stepanova, A.N., Robles, L.M., Lokerse, A.S., Alonso, J.M., Weijers, D., and Friml, J. (2013). Local auxin sources orient the apical-basal axis in *Arabidopsis* embryos. Curr. Biol. **23**: 2506–2512.

Ruzicka, K., Ljung, K., Vanneste, S., Podhorska, R., Beeckman, T., Friml, J., and Benkova, E. (2007). Ethylene regulates root growth through effects on auxin biosynthesis and transport-dependent auxin distribution. Plant Cell **19**: 2197–2212.

De Rybel, B., Audenaert, D., Beeckman, T., and Kepinski, S. (2009). The past, present, and future of chemical biology in auxin research. ACS Chem. Biol. **4**: 987–998.

Sato, S., Kato, T., Kakegawa, K., Ishii, T., Liu, Y-G., Awano, T., Takabe, K., Nishiyama, Y., Kuga, S., Sato, S., Nakamura Y., Tabata, S., and Shibat D. (2001). Role of the putative membrane-bound endo-1,4-beta-glucanase KORRIGAN in cell elongation and cellulose synthesis in *Arabidopsis thaliana*. Plant Cell Physiol. **42**: 251–263.

Sawchuk, M.G. and Scarpella, E. (2015). Control of vein network topology by auxin transport. BMC Biol. **13**: 94.

Simon, S., Kubeš, M., Baster, P., Robert, S., Dobrev, P.I., Friml, J., Petrášek, J., and Zažímalová, E. (2013). Defining the selectivity of processes along the auxin response chain: a study using auxin analogues. New Phytol. **200**: 1034–1048.

Simon, S. and Petrášek, J. (2011). Why plants need more than one type of auxin. Plant Sci. **180**: 454–460.

Song, Y. (2014). Insight into the mode of action of 2,4-dichlorophenoxyacetic acid (2,4-D) as an herbicide. J. Integr. Plant Biol. **56**: 106–113.

Steinwand, B.J., Xu, S., Polko, J.K., Doctor, S.M., Westafer, M., and Kieber, J.J. (2014). Alterations in auxin homeostasis suppress defects in cell wall function. PLoS One **9**: e98193.

Stepanova, A.N., Hoyt, J.M., Hamilton, A.A., and Alonso, J.M. (2005). A link between ethylene and auxin uncovered by the characterization of two root-specific ethylene-insensitive mutants in *Arabidopsis*. Plant Cell **17**: 2230–2242.

Stepanova, A.N., Robertson-Hoyt, J., Yun, J., Benavente, L.M., Xie, D.-Y., Dolezal, K., Schlereth, A., Jürgens, G., and Alonso, J.M. (2008). TAA1-mediated auxin biosynthesis is essential for hormone crosstalk and plant development. Cell **133**: 177–191.

Stepanova, A.N., Yun, J., Robles, L.M., Novak, O., He, W., Guo, H., Ljung, K., and Alonso, J.M. (2011). The *Arabidopsis* YUCCA1 flavin monooxygenase functions in the indole-3-pyruvic acid branch of auxin biosynthesis. Plant Cell **23**: 3961–3973.

Stone, S.L., Braybrook, S. A, Paula, S.L., Kwong, L.W., Meuser, J., Pelletier, J., Hsieh, T.-F., Fischer, R.L., Goldberg, R.B., and Harada, J.J. (2008). *Arabidopsis LEAFY COTYLEDON2* induces maturation traits and auxin activity: Implications for somatic embryogenesis. Proc. Natl. Acad. Sci. **105**: 3151–3156.

Stone, S.L., Kwong, L.W., Yee, K.M., Pelletier, J., Lepiniec, L., Fischer, R.L., Goldberg, R.B., and Harada, J.J. (2001). *LEAFY COTYLEDON2* encodes a B3 domain transcription factor that induces embryo development. Proc. Natl. Acad. Sci. USA **98**: 11806–11811.

Strader, L.C., Chen, G.L., and Bartel, B. (2010). Ethylene directs auxin to control root cell expansion. Plant J **64**: 874–884.

Su, Y.H. and Zhang, X.S. (2014). The hormonal control of regeneration in plants. Curr. Top. Dev. Biol. **108**: 35–69.

Swarup, R., Perry, P., Hagenbeek, D., Van Der Straeten, D., Beemster, G.T.S., Sandberg, G., Bhalerao, R., Ljung, K., and Bennett, M.J. (2007). Ethylene upregulates auxin biosynthesis in *Arabidopsis* seedlings to enhance inhibition of root cell elongation. Plant Cell **19**: 2186–2196.

Tao, Y. et al. (2008). Rapid synthesis of auxin via a new tryptophan-dependent pathway is required for shade avoidance in plants. Cell **133**: 164–176.

Ulmasov, T., Murfett, J., Hagen, G., and Guilfoyle, T.J. (1997). Aux/IAA proteins repress expression of reporter genes containing natural and highly active synthetic auxin response elements. Plant Cell **9**: 1963–1971.

Wójcikowska, B., Jaskóła, K., Gąsiorek, P., Meus, M., Nowak, K., and Gaj, M.D. (2013). *LEAFY COTYLEDON2* (*LEC2*) promotes embryogenic induction in somatic tissues of *Arabidopsis*, via *YUCCA*-mediated auxin biosynthesis. Planta **238**: 425–40.

Won, C., Shen, X., Mashiguchi, K., Zheng, Z., Dai, X., Cheng, Y., Kasahara, H., Kamiya, Y., Chory, J., and Zhao, Y. (2011). Conversion of tryptophan to indole-3-acetic acid by TRYPTOPHAN AMINOTRANSFERASES and YUCCAs in *Arabidopsis*. Proc. Natl. Acad. Sci. USA **108**: 18518–23.

Woodward, A.W. and Bartel, B. (2005). Auxin: regulation, action, and interaction. Ann. Bot. **95**: 707–735.

Zhao, Y., Christensen, S.K., Fankhauser, C., Cashman, J.R., Cohen, J.D., Weigel, D., and Chory, J. (2001). A role for flavin monooxygenase-like enzymes in auxin biosynthesis. Science 291: 306–309.

Zuo, J., Niu, Wu, Q.-W., Frugis, G., and Chua, N-H. (2002). The *WUSCHEL* gene promotes vegetative-to-embryonic transition in *Arabidopsis*. Plant J. **30**: 349–359.